

Fast-Response VHF Pulsed 2 KW Power Amplifiers

RICHARD W. QUINE,¹ GARETH R. EATON,¹ SHANE DILLON²

¹ Department of Engineering and Department of Chemistry and Biochemistry, Boettcher East Room 110, University of Denver, Denver, CO 80208-2436

² Tomco Technologies, Adelaide, South Australia

ABSTRACT: A pulsed power amplifier operating at a nominal 250 MHz with 2 kW (+63 dBm) output was designed to meet the specifications for an application in a pulsed EPR (electron paramagnetic resonance) spectrometer and was built by Tomco Technologies of Adelaide, South Australia. Key design features were pulse fidelity for short (e.g., 40 ns) RF pulses, output noise blanking after the pulse, and output power linear with input power from very low levels up to 2 kW output. A summary of the specifications, design, and performance of the amplifier is presented. The 2 kW RF amplifier tested has approximately 12 ns rise times and 15 ns fall times, permitting the formation of approximately 40 ns RF pulses. It has negligible amplitude droop over microsecond-long pulses and negligible phase change over microsecond long pulses. There was observable but small phase change during the rise and fall times of the pulse. Even for input pulses as short as 16 ns, the output pulse peaks at more than half of the rated power output. Application to measuring the free induction decays of triaryl methyl radicals in aqueous solution was demonstrated. © 2006 Wiley Periodicals, Inc. Concepts Magn Reson Part B (Magn Reson Engineering) 29B: 185–190, 2006

KEY WORDS: RF power amplifiers; pulsed EPR

INTRODUCTION

Pulsed EPR requires shorter pulses and shorter instrumental dead time than does pulsed NMR because electron spin relaxation times are many orders of magnitude shorter than nuclear spin relaxation times for many experiments of interest (1–3). In vivo EPR requires RF/microwave frequencies that are low relative to those traditionally used for EPR, and for the same reasons of tissue penetration overlap with fre-

quencies used for in vivo NMR spectroscopy and imaging (4). Consequently, one of the enabling technologies that needs to be developed for low-frequency pulsed EPR is pulsed RF amplifiers that amplify short pulses with good fidelity and then quickly blank the noise output after the pulse. Early development of our 250 MHz pulsed EPR spectrometer used a continuous-duty RF amplifier to achieve pulse fidelity, but this had the problem of continuous noise output that interfered with observing weak time-domain EPR signals (5). Subsequently, pulsed RF amplifiers were developed for this project. In a recent paper, it was reported that pulsed RF amplifiers at 250 MHz with up to 500 W output had achieved short (~40 ns) pulses and that the output noise was blanked to within 3 dB of thermal with a 40-ns transition time (6). Background literature was cited by Quine et al. (6). The amplifiers reported by Quine et al. (6) provided

Received 9 May 2006; revised 1 August 2006; accepted 1 August 2006

Correspondence to: R.W. Quine; E-mail: rquine@du.edu

Concepts in Magnetic Resonance Part B (Magnetic Resonance Engineering), Vol. 29B(4) 185–190 (2006)

Published online in Wiley InterScience (www.interscience.wiley.com). DOI 10.1002/cmr.b.20074

© 2006 Wiley Periodicals, Inc.

Table 1 Amplifier Specifications and Performance

Specification	Specified Value	Test Results
Center frequency	250 MHz	Met
Frequency bandwidth	± 10 MHz, 240–260 MHz, minimum	Met
Rise time	25 ns maximum, 10%–90% power	12 ns
Fall time	25 ns maximum, 90%–10% power	15 ns
Maximum blanked noise level	20 dB above thermal, 10 dB preferred	At or near the thermal limit ^a
Blanking transition	80 ns maximum	~100 ns, a low level transitional glitch was observed
Peak power level	2000 watts	2000 W linear, 2500 W saturated
Gain	Nominally 63 dB; 0 dBm input to produce full power output	Met
Linearity	± 1 dB from 40 dB below full power to full power	± 0.4 dB from 200 mW to 2 kW output
Phase droop	5 degrees maximum over 1 μ s pulse	Met
Duty cycle	2%	Met

^a Measurement was made using the bridge gain (and loss) to amplify the blanked noise level. Nominal gains and estimated losses were used in the calculations. The noise figures (NF) of the bridge amplifiers were not considered, but the first amplifier (+20 dB gain) has a NF of 0.5 dB.

sufficient power for use with small resonators (e.g., 1–2 cm diameter), but one goal is to apply in vivo electron paramagnetic resonance (EPR) spectroscopy and imaging to larger animals. Larger resonators will require higher power pulses to achieve 90-degree turning angles if the pulse length is kept the same. Consequently, the success of the 400 and 500 W amplifiers stimulated the further development of a 2-kW amplifier. The test results of this new amplifier are reported in this article. Although developed for pulsed EPR, the technology will be widely applicable in pulsed NMR also, especially solid-state NMR, which has short relaxation times.

MATERIAL AND METHODS

The most important performance specifications for the EPR application are given in Table 1, together with test results of these parameters. The amplifier was constructed by Tomco and tested at the factory and in the spectrometer in Denver.

Description of the Tomco Amplifier Design Approach

The following principles and specialized techniques were applied to optimize the amplifier's fast-pulse performance. The amplifier uses push-pull circuitry throughout.

When an RF pulse is applied to an amplifier, the DC current drawn by the power transistor increases approximately 10-fold, from its quiescent "bias" level

of typically 1 amp to its full power operating current of 10–15 amps. To achieve a rapid rise time, the amplifier must be designed in such a way that the path through which this current flows contains minimal series inductance. This is because inductance, by definition, opposes changes in current and thus limits the rise time. A push-pull power stage lends itself well to minimizing inductive effects because it provides a means of balancing antiphase currents by feeding the DC supply through a balanced "common-mode choke." This largely cancels the magnetic flux generated by the current flow, greatly reducing the effective series inductance.

Note that this cancellation occurs only if the two push-pull currents are exactly equal and opposite. Any imbalance or asymmetry in the circuit will result in imperfect cancellation and thus increase the rise time. For this reason, extreme care was taken in the PCB layout and in every aspect of the physical design to ensure near perfect balancing of currents in the push-pull circuitry.

To further minimize inductance or other impedances in the DC supply path, the large current that is drawn by the transistors during the RF pulse is drawn from storage capacitors located close to the power transistors. The storage capacitors chosen have extremely low internal inductance. In addition, multiple smaller capacitors are added in parallel with the main one, to ensure that the source impedance is low over a wide bandwidth.

The overall topology and gain distribution of the amplifier is designed to optimize its fast-pulse performance. High-power amplifiers are normally con-

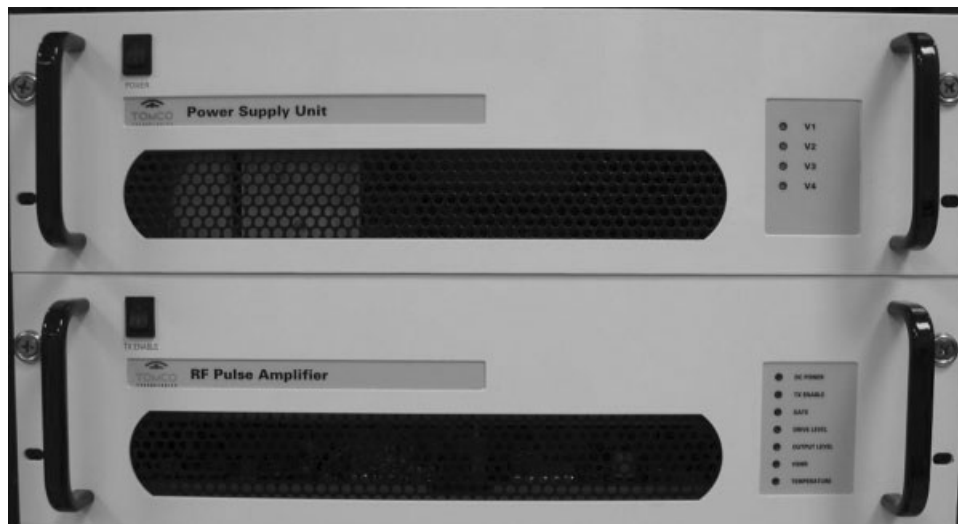


Figure 1 Tomco 2kW amplifier (bottom unit) with power supply (top unit). The power supply unit contains the first stage of RF amplification. Both units can be gated, but we found the best performance by gating only the second, high-power, portion of the amplifier.

structed using a high-gain input amplifier driving a number of single-stage high-power output amplifiers. In contrast, the new Tomco amplifier uses a low-power input amplifier driving multiple two-stage high-power output amplifiers. In other words, a greater proportion of the overall gain is located in the duplicated power stages. Although this technique involves considerably greater manufacturing cost than the usual method, it does permit much better matching between the driver and the high-power amplifiers. This reduces problems associated with ringing in matching circuits and reflections in RF drive cables.

The amplifier uses 32 independent two-stage power amplifier channels, or 64 power MOSFETs in total. In addition to this, the devices are operated at about half their rated power level so that they stay well within their linear region and away from saturation. Though this is not the cheapest way to build an RF power amplifier, it is the best way to ensure good fast-pulse performance.

A great deal of effort was put into making the design as physically compact as possible (Fig. 1). The goal was to minimize the length of interconnecting cables to minimize the duration of any reflections that may occur due to impedance mismatches between amplifier stages. It also minimizes the length of cables between the drive splitter and the power amplifiers, and again between the power amplifiers and the final power combiner. The design incorporates a two-level foldout shelf arrangement to achieve a compact construction without hampering serviceability (Fig. 2). Note that this design goal is facilitated somewhat by

the low duty-cycle specification for this amplifier, meaning that physically large heatsinks are not required.

Push-pull RF power MOSFETs are manufactured as a pair of separate transistor chips mounted on a single heatsink flange. Although the two transistors are tightly matched, there are always small differences in their electrical parameters. In particular, their threshold voltages can often be significantly different. In a conventional amplifier design, in which a single bias voltage is applied to both transistors, this difference in threshold voltages results in unequal current flow to each side of the device. This represents an imbalance which, as explained earlier, will ultimately limit the rise time. For this reason, a new bias gating circuit was developed to allow the push-pull currents to be accurately balanced. The new circuit uses a single-gated bias supply, which is split into two supplies with an adjustable offset voltage between them. This effectively provides two bias voltage pulses identical in every respect except for their offset. The offset is adjusted to compensate for threshold voltage differences and ensure perfect balancing of the push-pull currents.

For testing the amplifier with the spectrometer, pulses were generated by the Bruker E540 console with E-585 PatternJet 4-ns pulse programmer under control of the Bruker Xeptr software system. The 250-MHz bridge used was described in (5). Signals were digitized in a LeCroy 9354 500-MHz digital oscilloscope. To ensure that the pulse shapes are not affected by saturation of the amplifier output, the



Figure 2 Internal view of Tomco amplifier, showing the two-level foldout shelf arrangement.

pulse shapes were recorded in the linear region of the amplifier output.

The noise blanking was verified by measurement of the output in the blanked state with a true RMS voltmeter, Fluke model 8920A, after amplification by the bridge detection system. Transition time to the blanked state was observed by oscilloscope. For these measurements, the amplifier input was terminated with 50 ohms.

RESULTS

Figures 3–6 illustrate the pulse response performance of the amplifier. Figures 3 and 4 show the rising and falling edges of a 1 μ s output pulse. Because of the finite rise and fall times of the RF amplifiers, a pulse about 30 ns wide at half-power was created when the control signals were for a 40-ns pulse (see Fig. 5). The full output power was reached after approximately 60 ns, but a 40 ns pulse was attenuated by only about

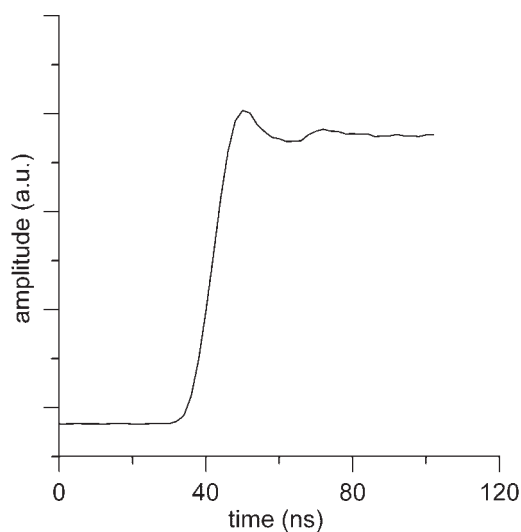


Figure 3 Leading edge of a 250-MHz 1- μ s pulse showing the 2-kW amplifier rise time of approximately 12 ns. The detector crystal gives an output proportional to power.

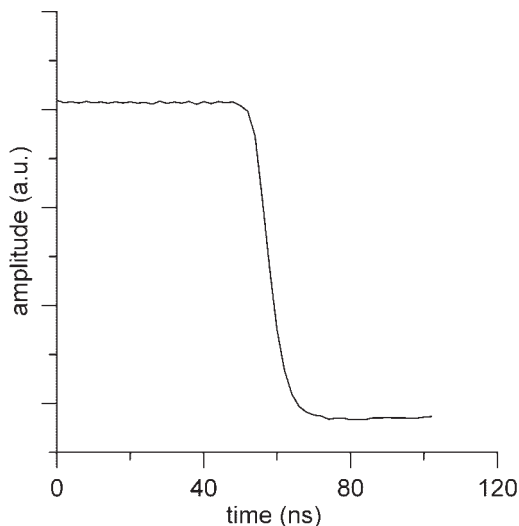


Figure 4 Trailing edge of 250-MHz pulse created by a 1 μ s control signal by the Tomco amplifier. The detector crystal yielded a display proportional to power.

10%. Because X-band (9–10 GHz) pulsed EPR commonly uses 16 ns pulses, the response of the 250 MHz amplifier to a 16-ns input pulse was measured (see Fig. 6). The 16-ns pulse rises to more half the full power, and is about 11 ns wide at half-height, but even this pulse, which is well outside the design range of the amplifier, is useful. The pulse shapes in the figures were recorded with minimal cable lengths from the attenuated output of the amplifier to a crystal detector in the spectrometer. The amplifier is extremely linear, yielding the same output pulse shapes

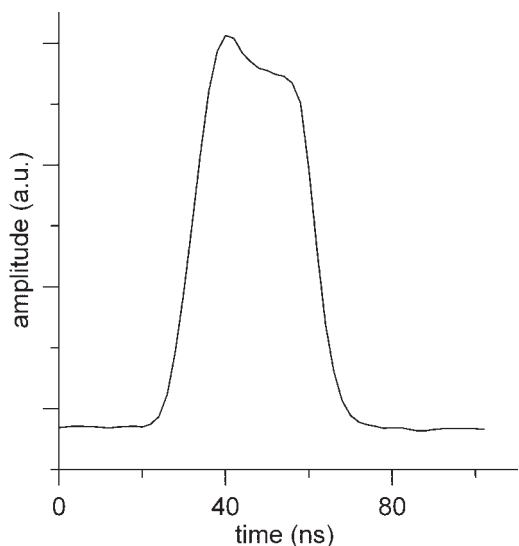


Figure 5 A 250-MHz 40-ns pulse output from the Tomco amplifier. The detector crystal yielded a display proportional to power.

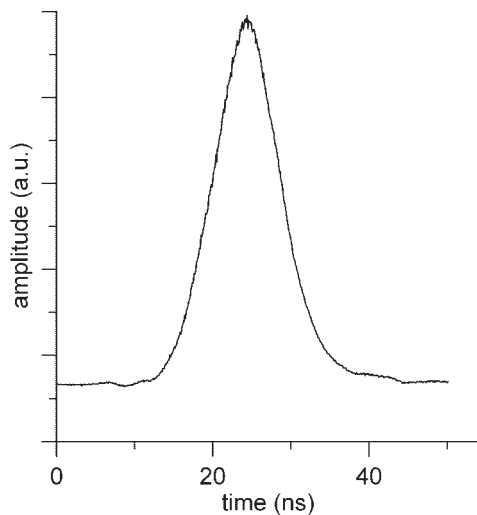


Figure 6 A 250-MHz pulse output from the Tomco amplifier created from a nominal 16-ns wide control signal. The detector crystal yielded a display proportional to power.

over a wide range of powers up to the design limit of 2000 W. Above 2000 W, to about 2500 W, the output is compressed. Small imperfections in the output pulse shape were shown to be the result of imperfections in the input pulses due to finite transition times of control switches and to video leakage caused by the fast transitions of control signals to the pulse-forming

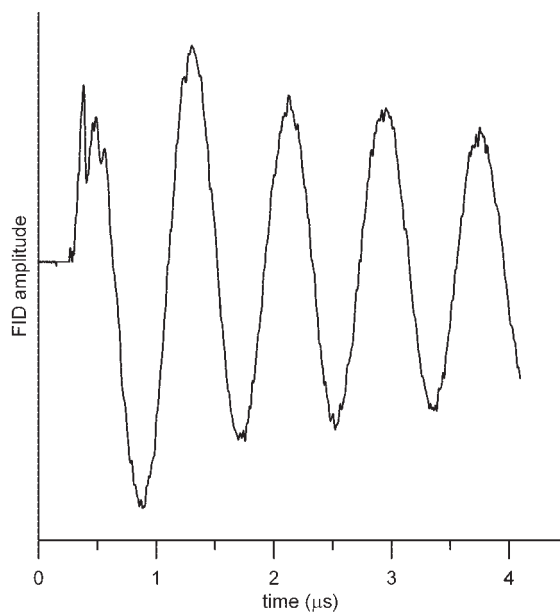


Figure 7 The free induction decay (FID) of a sample of triaryl methyl radical (trityl), following a 40-ns 90-degree RF pulse. An off-resonance background was subtracted. The flat line at early time is where both on- and off-resonance data were off-scale to the digitizer.

switches. Due to miscellaneous reflections, the pulse shape at the EPR sample resonator is somewhat different.

As a test of the practical dead time of the VHF spectrometer using the 2-kW RF amplifier, the free induction decay (FID) was measured of a sample of triaryl methyl radical (trityl). The sample was a 0.2-mM aqueous solution of the symmetric trityl containing $-CD_3$ groups (5, 7, 8). The sample was in a 10-mm o.d., 9-mm i.d. sample tube in the 25-mm diameter crossed-loop resonator previously described (9). Although this is a strong sample ($\sim 4 \times 10^{17}$ spins in the resonator), there is significant interference of instrumental artifacts with the FID for at least the first half microsecond. Most of this is due to the power ring down of the resonator after the high-power RF pulse. There is also some contribution from switching transients. The dead time is expected to be lower with lower Q resonators. Because the instrumental artifacts are independent of the sample, they are less important, and hence the practical dead time is lower, the stronger the EPR signal.

One of these amplifiers has been given extensive testing at the University of Denver, both as a stand-alone unit and as applied in the spectrometer application. A second copy of the amplifier is now entering service at the University of Chicago Center for EPR Imaging in Vivo Physiology.

SUMMARY

The 2-kW RF amplifier tested has approximately 12-ns rise times and 15-ns fall times, permitting the formation of approximately 40-ns RF pulses. It has negligible amplitude droop and phase change over microsecond-long pulses. There was observable, but small, phase change during the rise and fall times of the pulse. This pulsed RF amplifier is enabling technology for pulsed VHF EPR and will be useful in other fields requiring short RF pulses, such as solid-state NMR. The amplifier described in this article was

developed for the Center for EPR Imaging in Vivo Physiology, and is now commercially available from Tomco.

ACKNOWLEDGMENTS

This work was supported by NIH grant P41 EB002034 (Howard Halpern, PI), Center for EPR Imaging in Vivo Physiology.

REFERENCES

1. Eaton SS, Eaton GR. 2000. Relaxation times of organic radicals and transition metal ions. *Biol Magn Reson* 19:29–154.
2. Subramanian S, Krishna MC. 2005. Time-domain radiofrequency EPR imaging. *Biol Magn Reson* 23:321–383.
3. Subramanian S, Mitchell JB, Krishna MC. 2003. Time-domain radio frequency EPR imaging. *Biol Magn Reson* 18:153–197.
4. Halpern HJ, Bowman MK. 1991. Low-frequency EPR spectrometers: MHz range. In: Eaton GR, Eaton SS, Ohno K, editors. *EPR imaging and in vivo EPR*. Boca Raton, FL: CRC Press; chap. 6.
5. Quine RW, Rinard GA, Eaton SS, Eaton GR. 2002. A pulsed and continuous wave 250 MHz electron paramagnetic resonance spectrometer. *Magn Reson Eng* 15:59–91.
6. Quine RW, Eaton GR, Dillon S, Myer D. 2005. Fast-response VHF pulsed power amplifiers. *Concepts Magn Reson B (Magn Reson Eng)* 27B:1–7.
7. Yong L, Harbridge J, Quine RW, Rinard GA, Eaton SS, Eaton GR, et al. 2001. Electron spin relaxation of triarylmethyl radicals in fluid solution. *J Magn Reson* 152(1):156–161.
8. Owenius R, Eaton GR, Eaton SS. 2005. Frequency (250 MHz to 9.2 GHz) and viscosity dependence of electron spin relaxation of triarylmethyl radicals at room temperature. *J Magn Reson* 172:168–175.
9. Rinard GA, Quine RW, Eaton GR, Eaton SS. 2002. 250 MHz crossed loop resonator for pulsed electron paramagnetic resonance. *Magn Reson Eng* 15:37–46.